

# CHEMISTRY

---

## AN **ASIAN** JOURNAL

www.chemasianj.org

### Accepted Article

**Title:** USE OF P-SULFOCALIX[6]ARENE AS NANOCARRIER FOR DOXORUBICIN CONTROLLED DELIVERY

**Authors:** Pilar Lopez Cornejo, F.J. Ostos, J.A. Lebron, M.L. Moya, M. Lopez-Lopez, A. Sanchez, A. Clavero, C.B. Garcia Calderon, and I. del Valle Rosado

This manuscript has been accepted after peer review and appears as an Accepted Article online prior to editing, proofing, and formal publication of the final Version of Record (VoR). This work is currently citable by using the Digital Object Identifier (DOI) given below. The VoR will be published online in Early View as soon as possible and may be different to this Accepted Article as a result of editing. Readers should obtain the VoR from the journal website shown below when it is published to ensure accuracy of information. The authors are responsible for the content of this Accepted Article.

**To be cited as:** *Chem. Asian J.* 10.1002/asia.201601713

**Link to VoR:** <http://dx.doi.org/10.1002/asia.201601713>

A Journal of



A sister journal of *Angewandte Chemie*  
and *Chemistry* – A European Journal

---

WILEY-VCH

# USE OF P-SULFOCALIX[6]ARENE AS NANOCARRIER FOR DOXORUBICIN CONTROLLED DELIVERY

F. J. Ostos,<sup>[a]</sup> J. A. Lebrón,<sup>[a]</sup> M. L. Moyá, M.,<sup>[a]</sup> López-López,<sup>[b]</sup> A. Sánchez,<sup>[a]</sup> A. Clavero,<sup>[a]</sup> C.B. García-Calderón,<sup>[c]</sup> I.V. Rosado<sup>[c]</sup> and P. López-Cornejo<sup>[a]\*</sup>

**Abstract:** Given the high toxicity of the anthracycline antibiotic called doxorubicin (DOX), it is relevant to look for nanocarriers that, decreasing the side effects of the drug, were able to transport it towards a therapeutic target. Accordingly, the encapsulation of DOX by p-sulfocalix[6]arene (calix) has been studied. The interaction of DOX with the macrocycle, as well as with DNA, has been investigated and the equilibrium constant for each binding process estimated. Results showed that the binding constant of DOX to DNA,  $K_{DNA}$ , is three orders of magnitude higher than that to calix,  $K_{calix}$ . A multidisciplinary study has been done to demonstrate the ability of calixarenes to encapsulate DOX molecules, as well as the power of the DOX molecules included into the inner cavity of the macrocycle to bind with the DNA. Cytotoxicity measurements were done in different cancer and normal cell lines to probe the decrease in the toxicity of the encapsulated DOX, demonstrating thus the decrease of its side effects in the human organism. The low toxicity of calixarenes has also been demonstrated for different cell lines.

## 1. Introduction

Doxorubicin (DOX, Fig. 1A) is an anthracycline antibiotic with a high toxic character. The antitumor activity of this drug was discovered in the early 1960s and shows a wide spectrum of human cancers. DOX is used alone, or combined with other drugs, in the chemotherapeutic treatment of different solid tumors such as breast, ovarian and lung cancers as well as

in the treatment of leukemia and lymphomas.<sup>1-6</sup>

The action mechanism of DOX as anticancer drug is not well-known. Although the presence of different functional domains in the structure of this drug can produce diverse binding modes in the interaction DOX/DNA, the intercalation between nitrogen base pairs of the polynucleotide is the strongest binding mode and the cause of its cytotoxic effect. The intercalation of the drug results in the inhibition of the synthesis and transcription of the polynucleotide. It produces the blocking of an enzyme called topoisomerase II which inhibits the division and the growth of the cells. Besides, the intercalation of this drug in the DNA leads to changes in the chromatin structure: chromatin aggregation happens and this provokes the apoptotic of the cells.<sup>7-8</sup>

Despite of its beneficial antitumor activity, the clinical use of DOX is limited due to its side effects. As happens with other anticancer drugs, the use of DOX causes gastrointestinal toxicity. The patients treated with this anthracycline drug suffer vomiting, nausea and diarrhea after the treatment. Some patients suffer stomatitis within 7-10 days after the administration. High doses of DOX produce myelosuppression, which can lead to neutropenic fever and sepsis. Cardiotoxicity is another side effect produced by the use of this drug.<sup>9-12</sup>

In the last decade, diverse nanostructures have been used as vectors to encapsulate drugs. The objective of these works was to improve the transport of the drug towards its therapeutic target and, simultaneously, diminish its side effects. In this sense, perhaps liposomes are the more studied nanovectors for the delivery of doxorubicin. Storm et al. investigated the effect of the liposomes lipid composition on the antitumor activity of DOX.<sup>13</sup> Results showed that DOX entrapped in solid liposomes expresses a lower effective antitumor activity than when it is entrapped in fluid liposomes. Doxil® was the first lipid formulation containing DOX approved by FDA. A few years ago, Barenholz published an interesting review on the historical and scientific perspectives of Doxil, including the lessons learned from its development and its use for more than 20 years.<sup>14</sup>

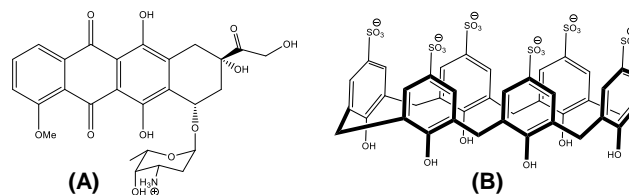


**Figure 1.** Structure of doxorubicin (A) and p-sulfocalix[6]arene (B).

Su et al. fabricated lipid-polymer nanoparticles based on the use of hydrophobic poly-(D,L-lactide-co-glycolide) as core, a hydrophilic poly(ethylene glycol) shell, and an interphase between these two layers composed by soybean phosphatidylcholine monolayer for co-delivery 2'-deoxy-5-azacytidine (DAC), an epigenic drug, and DOX.<sup>15</sup> The drugs were loaded in the core of the nanoparticles. Results showed that the presence of DAC significantly increased the sensibility

- [a] Mr. F.J. Ostos, Mr. J.A. Lebrón, Prof. M.L. Moyá, Dr. A. Sánchez, Mrs. A. Clavero, and Dr. P. López-Cornejo\*  
Departamento de Química Física, Facultad de Química  
Universidad de Sevilla  
c/ Prof. García González nº 1, Sevilla 41012, Spain  
E-mail\*: pcornejo@us.es
- [b] Dr. M. López-López  
Departamento de Ingeniería Química, Química Física y Ciencias de los Materiales, Facultad de Ciencias Experimentales  
Universidad de Huelva  
Campus 'El Carmen', E-21071, Spain
- [c] Dr. C.B. García-Calderón, Dr. Iván.V. Rosado  
Instituto de Biomedicina de Sevilla (IBiS)  
Hospital Universitario Virgen del Rocío/CSIC/Universidad de Sevilla  
Av. Manuel Siurot, s/n, 41013 Sevilla, Spain

For internal use, please do not delete. Submitted\_Manuscript

of cancer cells to DOX, inhibiting cell growth rate and inducing cell apoptosis.

Besides liposomes, other different vectors have been used for the transport and delivery of DOX. Mirza prepared gold nanoparticles<sup>16</sup> and, more recently, functionalized gold nanorods with folic acid with the same focus.<sup>17</sup> Results showed that the presence of folic acid favors the release of the drug, increasing the amount of DOX delivered to cancer cells. Dendrimers,<sup>18-20</sup> cyclodextrins,<sup>21,22</sup> micelles,<sup>23-25</sup> or carbon nanotubes<sup>26,27</sup> are also nanosystems used to carry DOX.

In the last years, calixarenes (calix) have been used as drug nanocarriers. A calix is a cyclic oligomer based on a hydroxialquilation product of an aldehyde and a phenol, resulting in cavities made of several phenolic units linked via methylene groups. Calixarenes have hydrophobic cavities that can hold smaller molecules.<sup>28,29</sup> They also show a hydrophilic character when the benzenes that form the ring are functionalized, either the *upper rim* or *lower rim* of the calix framework, with ionic groups.<sup>30,31</sup> Therefore, they contain both hydrophobic and hydrophilic compartments together in the same molecule.

Calixarene-based supramolecular vesicles have been constructed to be used as macrocyclic receptors, some of the investigation dealing with the encapsulation and release of DOX.<sup>32,33</sup> Cell experiments showed that the loading of the drug into the vesicles does not affect the therapeutic effect of DOX for cancer cells and, at the same time, the encapsulation diminishes the damage of the normal cells.

The design of nanovectors able to direct the drug to its target, maintaining its activity therapeutic but decreasing its side effect, results to be very important. Taking into account that both hydrophilic and hydrophobic regions of calixarenes can be systematically varied, the effects that these different calix structures produce on any drug can be investigated. Given the structural characteristics of these macrocycles, as well as their low toxicity, they are an ideal supramolecular system to be used as drug nanocarrier. Accordingly, a thorough study about the interaction of DOX with p-sulfocalix[6]arene molecules (see Figure 1B) have been done in this work. A negatively charged calix was chosen in order to favor the electrostatic interactions between DOX and calix since, at physiological pH, the DOX molecule is positively charged. The interaction between DOX and calf thymus DNA was also studied, as well as the effects that the addition of calix exerts on the binding of DOX with DNA. Finally, cell viability measurements were carry out to establish the therapeutic effect of the complex DOX/calix on different lines of cancer cells.

The results obtained in this work will contribute to the understanding of the drug/nanocarrier interactions, as well as of their therapeutic activity as a whole, which is paramount in order to develop new and more efficient nanovectors.

## 2. Results and Discussion

Given the complexity of the system studied, one ligand (guest) and two receptors (hosts), the interactions between the

different species are separately showed in order to clarify the work.

### 2.1. DOX-calix Interaction

DOX is an anthracycline antibiotic that shows absorption and emission spectra with peaks centered at 490nm and 554 nm, respectively. In our working conditions, the spectra obtained do not show any modification during more than one hour. This indicates that DOX is stable in buffer HEPES 40 mmol dm<sup>-3</sup> at pH=7.4.

The DOX absorption and emission spectra change when calix is added to the medium. Thus, the absorbance of the drug increases with the calix concentration, while the emission intensity decreases sharply in the presence of this receptor. Besides, a new band centered about 610 nm appears in the absorption spectrum at high calix concentrations (see Figure 2). These results indicate the existence of a clear interaction between calix and DOX molecules, with the formation of a new complex DOX/calix (an inclusion complex) in which, given their structures, the drug will be located into the hydrophobic inner cavity of the receptor.

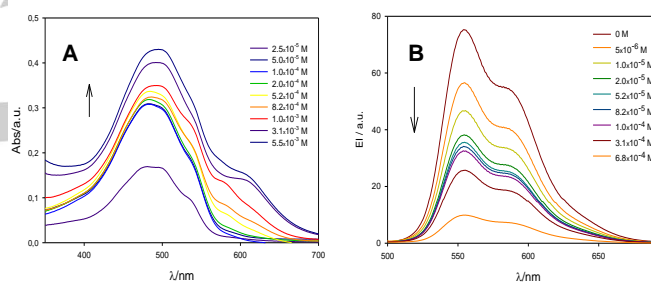


**Figure 2.** Absorbance (A) and emission (B) spectra of DOX at different calix concentrations.

In order to go further in the knowing of this inclusion complex, proton NMR measurements were carried out. Figure 3A shows the <sup>1</sup>H-NMR spectra of calix, DOX and calix/DOX (1:1) deuterated solutions at 298 K. These spectra show that interactions between calix and DOX molecules lead to considerable line broadening. Besides, a substantial decrease in the chemical shifts of most protons, either of the macrocycle or the antibiotic, is observed. Particularly, strong upfield shifts are shown by the signals corresponding to the aromatic protons H1, H2, and H3 of DOX (see the assignation of number for carbon atoms in Figure 3A). These variations in the <sup>1</sup>H-NMR spectrum can be rationalized by the shielding process due to the proximity of the calix aromatic rings when the antibiotic molecule goes into the macrocycle cavity. Favorable  $\pi$ - $\pi$  interactions would explain the larger chemical shifts found for the aromatic DOX protons, while the protons such as those to the sugar substituent are less affected. The large broadening of the signals precluded to carry out two-dimensional rotating frame nuclear Overhauser effect spectroscopy, ROESY, to get further information about the calix/DOX inclusion complex. The observed broadening seems to indicate that an equilibrium between different conformations of

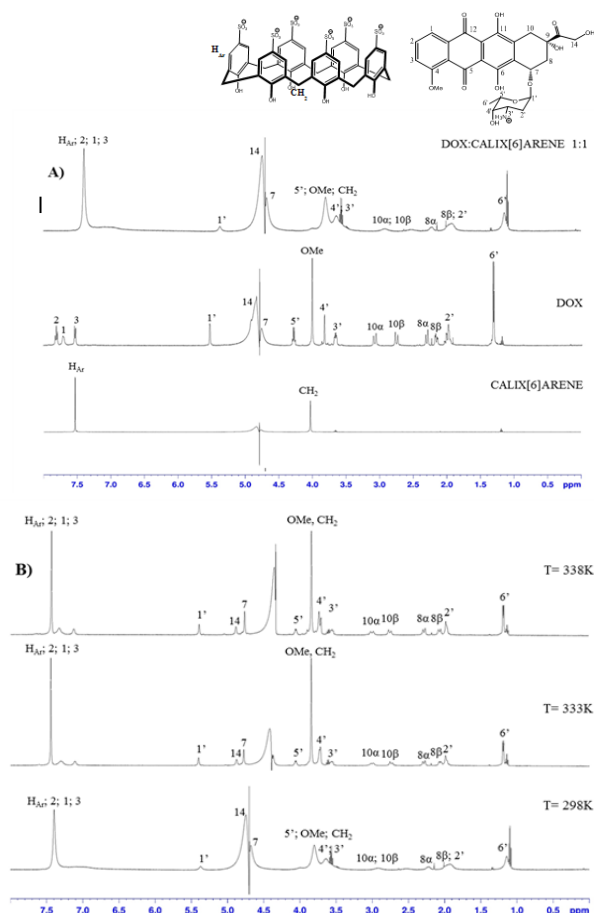


**Figure 3.** (A)  $^1\text{H-NMR}$  spectra of deuterated solutions of DOX, calix and a DOX:calix mixture (1:1) at  $298.0 \pm 0.1\text{K}$ . (B)  $^1\text{H-NMR}$  spectra of the 1:1 DOX:calix mixtures at different temperatures.

the inclusion complex exists. With the goal of investigating this possibility,  $^1\text{H-NMR}$  spectra were registered at higher temperatures, 333 and 338 K (it is worth noting that at these temperatures the deuterated solutions were stable for a limited time and ROESY measurements could not be done). One can see in Figure 3B, the lines get narrower when the temperature increases. In order to confirm the presence of chemical exchange processes, several proton NMR spectra were obtained at different magnetic fields. The results show a line broadening upon increasing the magnetic field strength, in agreement with dynamic processes such as chemical exchanges. These results support the hypothesis that an equilibrium process happened at our working conditions. The calix molecules can adopt different conformations due to the high flexibility of its structure, with the  $-\text{OH}$  and charged  $-\text{SO}_3^-$  groups alternatively located in the lower or in the upper rim of the macrocycle. With this in mind, the DOX molecules can go into the calixarene cavity through either of the rims. Once inside, the positively charged  $-\text{NH}_3^+$  group of DOX molecules can interact electrostatically with the negative charged  $-\text{SO}_3^-$  groups and  $\pi$ - $\pi$  interactions between the aromatic rings of the antibiotic and those of the calix will be at work. The contribution of one or

another interaction will depend on the position of the DOX molecules inside the cavity. The existence of several possible conformations for the DOX/calix inclusion complexes could explain the observed broadening of the NMR lines.

The stability of the inclusion complex can be described as:



where DOX and calix represent the free species in solution. In order to get information about the stoichiometry of the inclusion complex formed, the Job method was used.<sup>34</sup>

A series of solutions were prepared with different molar fractions of DOX and calix, maintaining always constant the total DOX+calix concentration. The absorbance and emission intensities of these solutions were measured at 490nm and 554 nm, respectively, the wavelengths of the maximum absorbance and emission intensity of the DOX complex in our working conditions. The values of  $[\text{DOX}]_x \Delta \text{Abs}$  (or  $\Delta \text{EI}$ ), where  $\Delta \text{Abs}$  (or  $\Delta \text{EI}$ ) are the increments observed in the absorbance (or in the emission intensity) when the molar fraction of calixarene increases from 0 to 1, were plotted versus the molar fraction of the drug (see Figure 4). The maximum of the plots gives information about the stoichiometry of the inclusion complex formed. Results indicate the formation of inclusion complexes of the type 1:1 (DOX:calix) for  $[\text{DOX}] < 1 \times 10^{-4} \text{ mol dm}^{-3}$ . For  $[\text{DOX}] > 1 \times 10^{-4} \text{ mol dm}^{-3}$  the average number of DOX molecules per inclusion complex is higher than 1, this indicating that some 2:1 complexes are formed. A possible explanation to this finding is

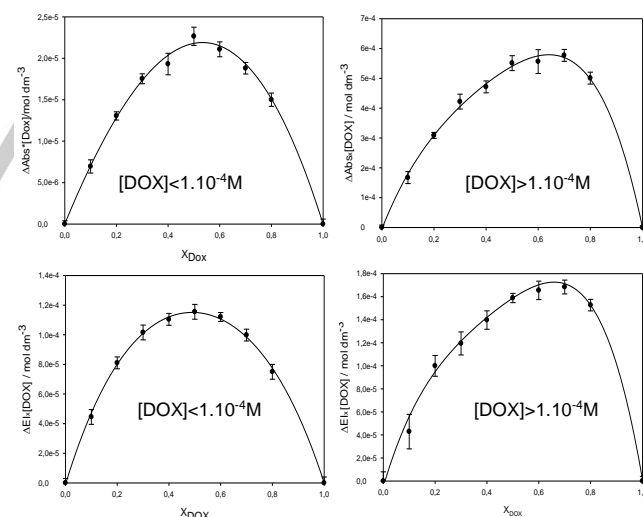


**Figure 4.** Job plots built from absorbance and emission data at DOX concentrations higher and lower than  $1.0 \times 10^{-4} \text{M}$ . Error bars represent standard deviations in each X value ( $n=5$ ).

that at high DOX concentration dimers of this drug are formed, as has been observed by Airoldi et al.<sup>35</sup> These dimers are the result of a stacking process, where  $\pi$ - $\pi$  interactions are operative between the planar aromatic rings of the DOX. The

For internal use, please do not delete. Submitted\_Manuscript

dimers could insert in the calix cavity or the stacking could happen between DOX molecules partially insert in the macrocycle. Nonetheless, bearing in mind that objective of this work is to use a well characterized nanovector to carry DOX, the rest of experiments were done at DOX concentration lower than  $1 \times 10^{-4} \text{ mol dm}^{-3}$ . The study of the interaction of dimers with this receptor will be done in a future.

The equilibrium constant  $K_{\text{calix}}$  corresponding to the formation of the DOX/calix complex (see eq. 1) can be obtained from the variations showed by the absorption and emission intensities when the calix concentration changes, by using the known pseudophase model proposed by Menger and Portnoy.<sup>36</sup> So, considering the distribution of the drug between the aqueous bulk and the inner cavity of the calix, one can write the following equation:

$$P/P_o = \frac{(P_w/P_o) + (P_{\text{calix}}/P_o) K_{\text{calix}} [\text{calix}]}{1 + K_{\text{calix}} [\text{calix}]} \quad (2)$$

where  $P/P_o$  is the relative property measured, absorption (Abs) or emission intensity (I), at different calix concentrations ( $P_o$  is the absorption or the emission intensity of DOX molecules in the absence of calix).  $P_w$  and  $P_{\text{calix}}$  are the absorption and emission intensities of the drug located in the aqueous (HEPES) solution and into the calix, respectively.  $[\text{calix}]$  is the total calix concentration added to the solution.  $K_{\text{calix}}$  is the equilibrium constant showed in equation 1 expressed as:

$$K_{\text{calix}} = \frac{[\text{DOX/calix}]}{[\text{DOX}_w] [\text{calix}_w]} \quad (3)$$

$[\text{DOX}_w]$  and  $[\text{calix}_w]$  being the free concentrations of DOX and calix, respectively, in the solution.

Absorption and emission data are well-fitted by using equation 2 as can be seen in Figure 5. The average  $K_{\text{calix}}$  value obtained from these fittings is  $(1.1 \pm 0.6) \times 10^5 \text{ mol}^{-1} \text{ dm}^3$  that demonstrates a strong interaction between DOX and calix. This equilibrium constant has also been obtained from circular dichroism and cyclic voltammetry measurements (see electronic supplementary information). The values obtained were  $(8.3 \pm 0.3) \times 10^4 \text{ mol}^{-1} \text{ dm}^3$  and  $(1.2 \pm 0.2) \times 10^5 \text{ mol}^{-1} \text{ dm}^3$ , respectively.

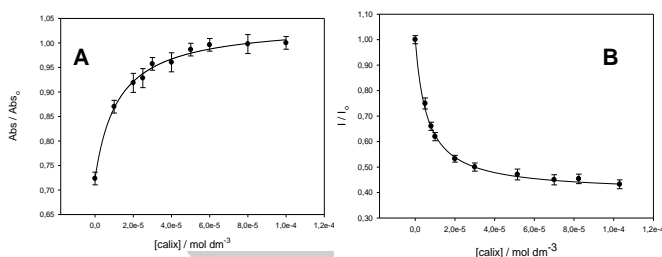


**Figure 5.** Plots of relative absorbance (A) and emission intensities (B) of DOX versus total calix concentration at 490nm and 550nm, respectively. Points represent experimental data. Lines show the best fits obtained by using equation 2. Error bars represent standard deviations in each X value ( $n=5$ ).

## 2.2. DOX-DNA Interaction

Several authors have studied the interaction between DOX and DNA. Recently, Pérez-Arnaiz *et al.* have studied the mechanism of interaction DOX-DNA.<sup>37</sup> According to their results, two different complexes are formed depending on the molar ratio  $[\text{DOX}]/[\text{DNA}]$  present in the solution. The authors have assumed that the formation mechanism of the DOX/DNA complex happens in two steps: a first (fast) step in a groove mode in the AT regions and a second (slow) step of intercalation in the GC regions. On the contrary, Airoldi *et al.* did not find any affinity of DOX for AT or GC sites.<sup>35</sup> With the aim of investigating the DOX/DNA interactions under our working conditions, circular dichroism measurements were carried out.

DNA solutions show a typical spectrum in the wavelength range 200-320 nm with a negative band centered at 248 nm, due to the helical structure of the polynucleotide; and a positive band centered at 280 nm, due to the base stacking. The addition of DOX to a DNA solution provokes changes in the CD spectrum of the polynucleotide. Results shows that initially the addition of DOX causes an increase of the positive band at 280 nm, up to a determined DOX concentration (a molar ratio  $X = [\text{DOX}]/[\text{DNA}] \sim 0.25$ ). Further additions of DOX provoke hypochromic and hypsochromic effects of this positive band (see Fig. 6A). On the contrary, the negative peak of the spectrum always increases upon increasing DOX concentration (see Figures 6B and 6C). It must be noted that the band centered at 300nm observed in the dichroism spectrum and the wide band obtained in the visible spectral region are due to the formation of a DOX/DNA complex (all CD spectra are run using a solution of HEPES  $40 \text{ mmol dm}^{-3}$  that contains the DOX concentration required for each X value as reference solution). The isosbestic point registered at 330 nm confirms the formation of a DOX/DNA complex, which is in agreements with previous results.<sup>35,37</sup>

Viscosity measurements can also be used for getting information about the formation of DOX/DNA complexes. Figure 7 shows that an increase in the relative viscosity value is observed when  $[\text{DOX}]$  increases, up to a molar ratio about 0.25. From that X value, the relative viscosity of the solution decreases. It is known that the intercalation of a probe into the base pairs of the DNA leads to an increase of the polynucleotide length and, therefore, an increase in the viscosity of the solution.<sup>37</sup> Results in Figure 7 can be explained by considering that, at low X values, the DOX molecules intercalate into the DNA base pairs forming DOX/DNA complexes and augmenting the viscosity. When the DOX concentration increases, the antibiotic molecules form dimers, which can cause the partial leaving of the intercalated DOX molecules. Accordingly, the polynucleotide length diminishes and this results in a decreasing of the solution viscosity. This also explains the hypsochromic and hypochromic effects obtained in the CD spectra.

The binding of DOX to DNA can also be studied from fluorescence measurements using the Scatchard plot.<sup>38</sup> This graphical method permits to analyze the type of binding of a ligand with a receptor, such as DNA, that contains different binding sites. In this way, the average number of DOX

molecules bound per DNA molecules can be estimated from fluorescence data plotting the concentration ratio of bound DOX to unbound DOX versus the bound antibiotic concentration ( $v$ ). Figure 8A shows the Scatchard plot obtained. In this case a linear trend is not observed. On the contrary, a concave-down curve is seen. This behavior indicates a positive cooperative character of the interaction of DOX with DNA, which is in agreement with the fact that different binding modes are acting in the interaction DOX-DNA.<sup>39</sup>

where:

$$K_{\text{DNA}} = \frac{K_{\text{max}}^{\text{DNA}} e^t}{1 + e^t} \quad (5) \quad t = \frac{[\text{DNA}] - h}{j} \quad (6)$$

$K_{\text{max}}^{\text{DNA}}$  being the maximum (limiting) value of  $K_{\text{DNA}}$ ,  $h$  the value of  $[\text{DNA}]$  for which  $K_{\text{DNA}} = (1/2)K_{\text{max}}^{\text{DNA}}$  and  $j$  an adjustable parameter.  $I_w$  is the emission intensity of free DOX molecules located in the aqueous (buffered) solution and  $I_{\text{DNA}}$  is the emission intensity of the DOX molecules bound to the polynucleotide.  $I_0$  is the emission intensity of DOX molecules in the absence of DNA.

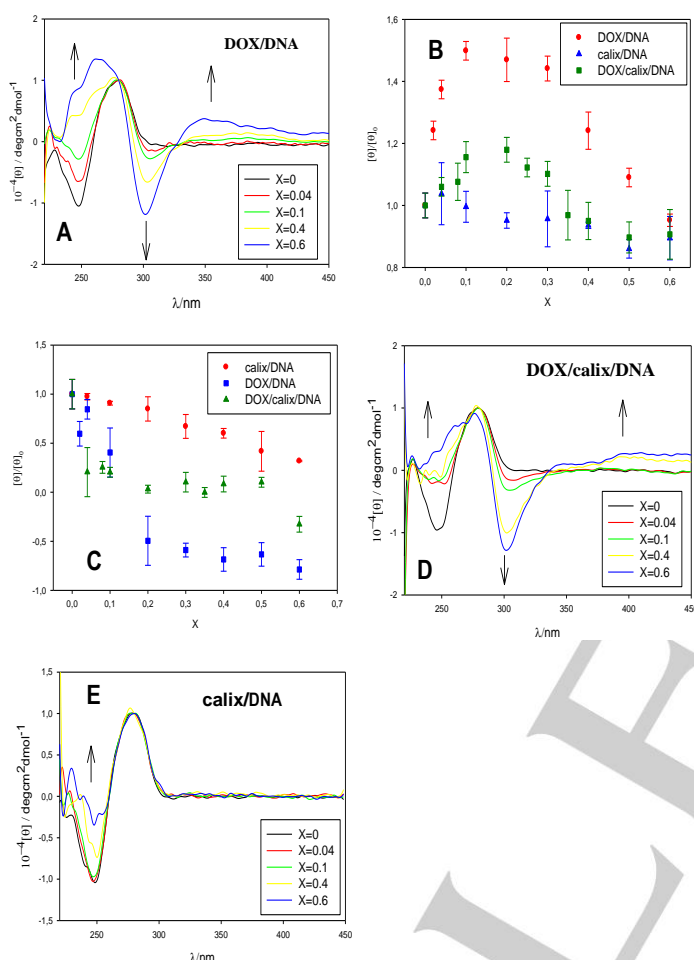


**Figure 6.** Circular dichroism spectra of DOX/DNA (A), DOX/calix/DNA (D) and calix/DNA (E). Relative molar ellipticity data obtained at  $\lambda=280\text{nm}$  (B) and  $\lambda=248\text{nm}$  (C) for different X values ( $X=[\text{DOX}]/[\text{DNA}]$  in plots A-D and  $X=[\text{calix}]/[\text{DNA}]$  in plot E). Error bars represent standard deviations in each X value ( $n=10$ ).

The average binding constant corresponding to this interaction can be estimated by using a modification of the pseudophase model, considering a sigmoidal dependence of the equilibrium constant on the DNA concentration. This procedure has been previously used for other binding processes.<sup>40</sup> Bearing this in mind one can write the following equation for the relative emission intensity of the DOX:

$$I/I_0 = \frac{(I_w/I_0) + (I_{\text{DNA}}/I_0) K_{\text{DNA}} [\text{DNA}]}{1 + K_{\text{DNA}} [\text{DNA}]} \quad (4)$$

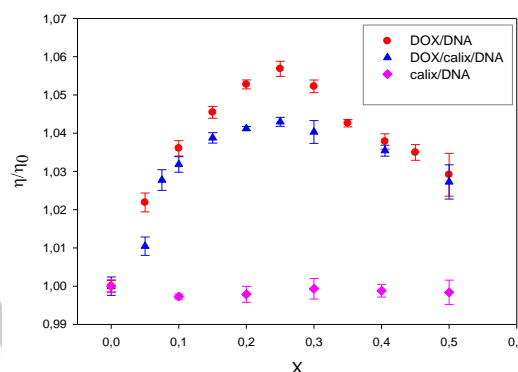


**Figure 7.** Relative viscosity of DOX/DNA, calix/DNA and DOX/calix/DNA solutions at different X values. Error bars represent standard deviations in each X value ( $n=10$ ).

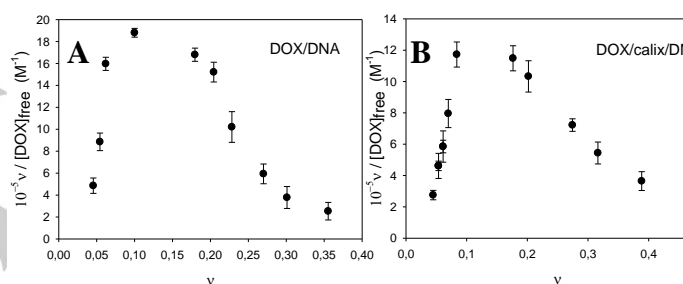


**Figure 8.** Scatchard plot of DOX/DNA (A) and DOX/calix/DNA (B). Error bars represent standard deviations in each X value ( $n=5$ ).  $[\text{DOX}] = 6.0 \times 10^{-6} \text{ mol dm}^{-3}$ ,  $[\text{calix}] = 5.0 \times 10^{-5} \text{ mol dm}^{-3}$ .

Figure 9 shows that there is a good agreement between the theoretical and the experimental data by using equations 4-6 for the fittings. In this case a value of  $K_{\text{max}}^{\text{DNA}} = (6.6 \pm 1.1) \times 10^8 \text{ mol}^{-1} \text{ dm}^3$  is obtained, which is according with the binding constant obtained by other authors.<sup>37</sup>

The fact that  $K_{\text{max}}^{\text{DNA}}$  is three orders of magnitude higher than  $K_{\text{calix}}$  is a good starting point to research our main goal, the use of calix as carrier of the antibiotic towards DNA. Taking into account that  $K_{\text{max}}^{\text{DNA}} \gg K_{\text{calix}}$ , one would expect that the DOX molecules encapsulated in the macrocycle will leave the hydrophobic cavity when the polynucleotide is added to the medium, preferentially interacting with it and, therefore, fulfilling its therapeutic activity.

For internal use, please do not delete. Submitted\_Manuscript

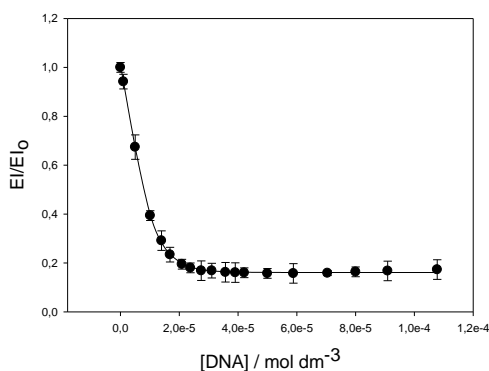


**Figure 9.** Titration of DOX with DNA. Points represent experimental data. Line shows the best fitting according to equations 4-6.  $[DOX]=5.0 \times 10^{-6} \text{ mol dm}^{-3}$ . Error bars represent standard deviations in each DNA concentration ( $n=6$ ).

### 2.3. DOX-calix-DNA Interaction

CD spectra of DNA in the presence of the DOX/calix complex were run for different X molar ratio ( $X=[DOX]/[DNA]$ ,  $[DOX]$  being the total concentration of drug added to the solution). The concentrations of calix and DNA were maintained constant in all the measurements and the DOX concentration is always lower than  $1.0 \times 10^{-4} \text{ mol dm}^{-3}$  in order to avoid the formation of dimers. Figure 6D presents the CD spectra obtained for different X values. Comparing Figures 6A and 6D, a similar change of the DNA spectrum in the presence of DOX and in the presence of the DOX/calix complex is observed. From Figures 6B and 6C one can compare the differences obtained in the peaks centered at 280 nm and at 248 nm, respectively, in the presence and absence of calix. Although the behavior is similar, and the maxima appear at the same X values, changes in ellipticity values are reduced in the presence of the calix. This points out that some DOX molecules, the free DOX molecules that are not located into DNA, are included into the receptor cavity. This behavior diminishes the negative side effects that an excess of the free antibiotic exerts in the human organism. The negative band centered at 248 nm also disappears in the presence of calix, but the variations are not as drastic as in the absence of the nanocarrier.

The effect that the calix exerts by itself in the polynucleotide has also been studied by CD measurements. No new band, or induced band, due to the presence of calix is observed. However, its presence slightly modifies the DNA spectrum. As is observed in Fig 6E, the positive band of DNA does not practically change but the negative band suffers a decrease in the ellipticity value. Therefore, the helical structure of the polynucleotide is slightly modified. This result, although surprising given the repulsive electrostatic interaction between calix and DNA due to negative charges of both species (sulfonic groups in calix and phosphate backbone in DNA), demonstrates that a certain interaction takes place between calix and DNA, probably in a groove mode (minor and/or mayor groove). Taking into account the structure of the calix used (see Figure 1B), the interaction between these species would take place by the neutral side of the calix, that is, through the side of the -OH

groups. In any case, the non-rigid structure of the calix must also be considered. In fact, the mobility of its structure permits to find several conformations of the macrocycle in the solution. This could assist the approach of the calix to the DNA helix.

The interaction between the receptor (calix) and the polynucleotide benefits the goal of this work. The tendency showed by the calix to localize by itself close to the DNA helix makes the approach of DOX molecules to the polynucleotide more favorable.

Viscosity data obtained with the DOX/calix/DNA solution are according to results obtained from CD spectra (see Fig 7). The viscosity increases at low X values and decreases for larger molar ratios. Again, a maximum point is observed at an X value about 0.2 as happens in the absence of calix. However, the variation obtained in the viscosity data with X is smaller. This indicates that the free DOX molecules that are not intercalated into the nitrogen pair bases of DNA are not located in the solution. On the contrary, these are placed into the cavity of the calix, which acts as a nanocarrier.

Viscosity data of the calix/DNA solution were also measured to prove the interaction of calix with the polynucleotide. Figure 7 shows a slight decrease of the viscosity by increasing the concentration of calix in the medium (in this case X is defined as  $[calix]/[DNA]$ ). This result supports the idea that calix binds slightly with DNA by a (minor and/or major) groove mode.

The presence of calix in the medium does not modified the positive cooperative character of the interaction DOX/DNA. In fact, a concave-down curve is again observed in the Scatchard plot in the presence of calix (see Figure 8B).

The potential toxic effects that DOX, calix and the DOX/calix complex exert on different cancer cell lines have been studied. Results on the viability of cell growth are recorded in Figure 10A. Data show the low toxicity of calix at low concentrations for the five cell lines used (see Fig. 10A). Only a slight toxicity has been observed at the highest concentrations. Practically there is not difference in the toxicity of the calix in most of the cell lines studied. The human lung cancer cell line H358 is slightly the less affected by the presence of the macrocycle, while the liver cancer cell line HepG2 is the most affected. In any case, the toxicity produced by the nanocarrier is very small for the lower concentrations of the macrocycle. This result demonstrates that calixarenes could be used as nanovectors in nanomedicine.

Bearing all these results in mind, viability measurements of DOX and DOX/calix are made for the different cancer cell lines LS180, MCF7, A549, H358 and HepG2 at distinct measurement times (24h, 48h, 72h and 96h). Figures 10B-F and S5-S9 summarize the results obtained. It is observed that the presence of calix decreases the toxicity of DOX for most variety of cell lines. Only in the human liver cancer cell line (HepG2), a decrease in the toxicity of DOX located into the cavity of calix is observed for the lowest calix concentrations (up to  $10 \times 10^{-6} \text{ M}$ ). An increase in the toxicity (higher than the produced by DOX

For internal use, please do not delete. Submitted\_Manuscript

alone) is obtained for macrocycle concentrations higher than  $25 \times 10^{-6}$  M in the HepG2 cell line. Remember that the toxicity of calix is higher for the HepG2 line than for the rest of lines. In this case the toxicity of calix will be added to that produced by DOX, resulting in a higher toxicity of the DOX/calix complex. The measurement time does not affect after 72h (24h and 48h seem not to be sufficient to happen the cellular division and observed the effect of the antibiotic-see ESI).

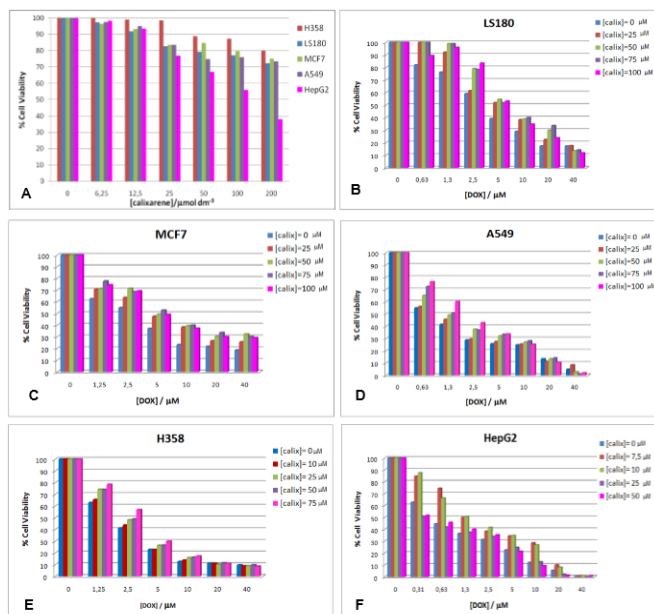


**Figure 10.** (A) % cell viability in the presence of different calix concentrations. (B-F) Cytotoxicity of DOX in the presence and absence of calix for different cancer cell lines at a measurement time of 96h.

Assays of cytotoxicity were also done with the normal cell line RPE-1 (retinal epithelial cell) (see Figure S10 in ESI). The same results that for the cancer cells were obtained: the calixarene does not produce any toxic effect on the cells and the presence of calixarene decrease the toxicity of the DOX.

### 3. Conclusions

It has been demonstrated that calixarenes can act as good hosts to encapsulate doxorubicin. The fact that p-sulfocalix[6]arene has preference for locating close to the DNA structure, in a groove position given the CD spectra obtained, facilitates the transport of the antibiotic towards the polynucleotide (see Figure 11). Besides, cytotoxicity results demonstrate that the presence of calix in the solution partially reduces the side effects that DOX provokes in the human organism. Only in the case of the liver cancer cell line (HepG2), the concentration of the nanocarrier used must be low in order to decrease such side effects.

Given the low toxicity demonstrated by calixarenes and their use in drug delivery, they must be accepted to be used with pharmacological purposes.

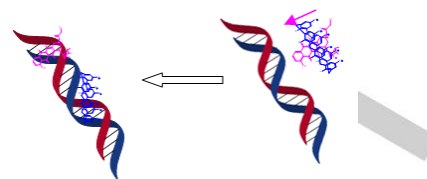


**Figure 11.** Pictorial representation of the interaction DOX/calix/DNA.

## Experimental Section

### Materials

Doxorubicin was obtained from Sigma-Aldrich. p-sulfonocalix[6]arene sodium salt and DNA calf thymus were purchased from Alfa-Aesar and Fluka, respectively. All reactants were of analytical grade (P.A.) and used without further purification. The solutions were prepared with distilled and deionized water, obtained of a Millipore Milli-Q system, with a conductivity  $\leq 10^{-6}$  S m<sup>-1</sup>. The pH of the solutions was maintained constant at a value of 7.4 by using a buffer HEPES (4-(2-hydroxyethyl)piperazine-1-ethanesulfonic acid sodium salt) of concentration 40 mmol dm<sup>-3</sup>. The whole measurements were done at  $303.0 \pm 0.1$  K.

### Methods

#### Absorbance Measurements

Absorbance spectra were performed to check the stability of the different solutions. Absorption spectra were run in a Cary 500 SCAN UV-vis-NIR (Varian). Quartz cells of 10 mm path length were used. Data were collected every 1 nm and spectra were recorded in the wavelength range from 200 to 700 nm.

#### Fluorescence measurements

Emission Intensity measurements were carried out in a Hitachi-f-2500 spectrofluorimeter interfaced to a PC for the recording and handling of the spectra. Standard fluorescence quartz cell of 10 mm path length was used. Fluorescence titrations were performed at a fixed DOX concentration of  $7.8 \times 10^{-5}$  mol dm<sup>-3</sup> and different DNA and/or calixarene concentrations: [calix]=0- $5.5 \times 10^{-3}$  mol dm<sup>-3</sup> and [DNA]=0- $1.0 \times 10^{-5}$  mol dm<sup>-3</sup>. The excitation and emission wavelengths used were 490 nm and 550 nm respectively.

#### Viscosity measurements

Viscosity measurements were carried out using an Ostwald viscosimeter immersed in a thermostated water bath at a temperature of  $303.0 \pm 0.1$  K. The viscosimeter was calibrated with water and ethanol. The measurements were repeated at least ten times.

The viscosity behavior of the DOX/DNA, Calix/DNA and DOX/Calix/DNA solutions was characterized through the relative viscosity  $\eta_r$ , defined as  $\eta/\eta_0$ , that is, the ratio between the viscosity of the solution and the viscosity of the pure solvent (HEPES 40 mmol dm<sup>-3</sup> at pH=7.4). The dependence that  $\eta_r$  shows with the molar ratio [DOX]/[DNA] gives information about structural changes in the polynucleotide.

Viscosity measurements were done at fixed DNA and Calix concentrations ([DNA]= $1.0 \times 10^{-4}$  mol dm<sup>-3</sup> and [calix]= $5.0 \times 10^{-5}$  mol dm<sup>-3</sup>). The DOX concentration was changed in order to study the molar ratio [DOX]/[DNA] desired.

#### Circular dichroism spectra

Electronic circular dichroism (CD) spectra were recorded in a Biologic Mos-450 spectropolarimeter. A standard quartz cell of 10 mm path length was used. Scans were taken from 220 to 450 nm. Each spectrum was obtained from an average of 10 runs at a fixed temperature of  $303.0 \pm 0.1$  K with a 5 min equilibration before each scan. The spectra obtained were expressed in terms of molar ellipticity,  $[\Theta]$ .

Spectra were performed at fixed DNA and calix concentrations and in the presence of varying amounts of doxorubicin in order to obtain the appropriate molar ratio X. The concentrations of DNA and calixarene used were  $1.0 \times 10^{-4}$  mol dm<sup>-3</sup> and  $5.0 \times 10^{-5}$  mol dm<sup>-3</sup>, respectively.

#### <sup>1</sup>H-NMR spectra

Proton NMR spectra were performed in CITIUS (Research General Services for the University of Seville). NMR samples were prepared by dissolving the corresponding amount of DOX and/or calix in D<sub>2</sub>O followed by a brief sonication. The solutions were kept at  $298.0 \pm 0.1$  K for at least 5 hours before carrying out the NMR experiments. NMR experiments were recorded on a Bruker Avance III 500 MHz spectrometer (500.2 MHz for <sup>1</sup>H) equipped with a 5 mm TCI cryoprobe operating at  $298.0 \pm 0.1$  K. All <sup>1</sup>H chemical shifts are referenced to the residual HDO signal set to 4.71 ppm.<sup>41</sup> The assignment of number for carbon atoms used is the same than that given by other authors.<sup>42</sup>

#### Electrochemical measurements

Electrochemical measurements were performed using an EC Epsilon potentiostat (BASi). Cyclic voltammetry measurements were run with a three electrode system containing a platinum foil as the counter electrode, a silver/silver chloride (Ag/AgCl) electrode as the reference electrode and a glassy carbon electrode of 3mm diameter (Model CHI104, CH Instruments) as the working electrode. All data were recorded at  $303.0 \pm 0.1$  K and in a Hepes 40mM buffer.

#### In vitro cytotoxicity assays

In order to measure DOX sensitivity, cytotoxicity measurements in vitro were done by using a MTT assay.<sup>43</sup> Cell lines were plated out into 96 well plates at a density of 3000 cells per plate. Five human cancer cell lines were used: A549 (adenocarcinomic human alveolar basal epithelial cell line), H358 (human lung cancer cell line), HepG2 (human liver cancer cell line), LS180 (adenocarcinomic human colonic epithelial cell line) and MCF7 (breast cancer cell line); and a normal cell line: RPE-1. Next day, different doses of DOX were added to wells and the plate returned to the incubator for four days more. The medium was supplemented with different doses of calixarene. Following this, they were pulsed with MTS (ROCHE). Cell viability was measured by luminometry according to manufacturer's instructions. Each dose point was measured in triplicate.

## Acknowledgements

This work was supported by the Consejería de Educación y Ciencia de la Junta de Andalucía (Proyecto de Excelencia P12-FQM-1105, FQM-206 and FQM-274) and the European Union (Feder Funds). The authors thank the University of Seville for the grant VPPI-US. IVR is a recipient of a Miguel Servet contract (CP12/03273) from Instituto de Salud Carlos III (PI15/01409).

**Keywords:** Doxorubicin • nanocarrier • DNA • chemotherapeutic treatment • drug controlled delivery.

- [1] J.H. Edmonson, L.M. Ryan, R.H. Blum, J.S. Brooks, M. Shiraki, S. Frytak, D.R. Parkinson, *J. Clin. Oncol.* **1993**, *11*, 1269-1275.
- [2] P. Lutwyche, C. Cordeiro, D.J. Wiseman, M. St-Louis, M. Uh, M.J. Hope, M.S. Webb, B.B. Finlay, *Antimicrob. Agents Chemother.* **1998**, *2511-2520*.
- [3] K.M. Laginha, S. Verwoert, G.J.R. Charrois, T.M. Allen, *Clin. Cancer Res.* **2005**, *11*, 6944-6949.
- [4] M. Harada, I. Bobe, H. Saito, N. Shibata, R. Tanaka, T. Hayashi, Y. Kato, *Cancer Sci.* **2011**, *102*, 192-199.
- [5] P. Weber, M. Wagner, H. Schneckenburger, *Int. J. Mol. Sci.* **2013**, *14*, 8358-8366.
- [6] Y. Zhang, C. Yang, W. Wang, J. Liu, Q. Liu, F. Huang, L. Chu, H. Gao, C. Li, D. Kong, Q. Liu, J. Liu, *Scientific Reports* **2016**, *6*, 1-12.
- [7] T.R. Dunkern, I. Wedemeyer, M. Baumgärtner, G. Fritz, B. Kaina, *DNA Repair* **2003**, *2*, 49-60.
- [8] E.J. Walsby, S. J. Coles, S. Knapper, A.K. Burnett, *Haematologica* **2011**, *96*, 393-399.
- [9] J.W. Cowens, P.J. Creaven, W.R. Greco, D.E. Brenner, Y. Tung, N. Petrelli, *Cancer Res.* **1993**, *53*, 2796-2802.
- [10] E.A. Lefrak, J. Pitha, S. Rosenheim, J.A. Gottlieb, *Cancer* **1973**, *32*, 302-314.
- [11] B.K. Sinha, E.G. Mimnaugh, *Free Radical Biol. Med.* **1990**, *8*, 567-581.
- [12] J.E. Wortman, V.S. Jr. Lucas, E. Schuster, D. Thiele, G.L. Logue, *Cancer* **1979**, *44*, 1588-91.
- [13] G. Storm, F.H. Roerdink, P.A. Steerenberg, W.H. de Jong, D.J.A. Crommelin, *Cancer Research* **1987**, *47*, 3366-3372.
- [14] Y.C. Barenholz, *J. Controlled Release* **2012**, *160*, 117-134.
- [15] X. Su, Z. Wang, L. Li, M. Zheng, C. Zheng, P. Gong, P. Zhao, Y. Ma, Q. Tao, L. Cai, *Mol. Pharmaceutics* **2013**, *10*, 1901-1909.
- [16] A.Z. Mirza, H. Shamshad, *Eur. J. Med. Chem.* **2011**, *46*, 1857-1860.
- [17] A.Z. Mirza, *J. Drug Target* **2015**, *23*, 52-58.
- [18] I.-H. Lee, M.K. Yu, I.H. Kim, J.-H. Lee, T.G. Park, S. Jon, *J. Controlled Release* **2011**, *155*, 88-95.
- [19] H. Yang, *Pharm. Res.* **2010**, *27*, 1759-71.
- [20] J.-T. Lin, Y. Zou, C. Wang, Y.-C. Zhong, Y. Zhao, H.-E. Zhu, G.-H. Wang, L.-M. Zhang, X.-B. Zheng, *Mat. Sci. Eng.: C* **2014**, *44*, 430-439.
- [21] A. Al-Omar, S. Abdou, L. De Robertis, A. Marsura, C. Finance, *Bioorg. Med. Chem. Lett.* **1999**, *9*, 1115-1120.

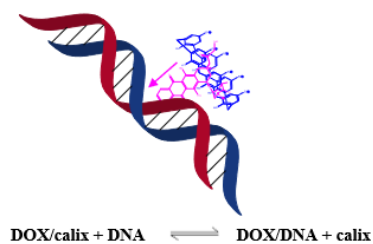
- [22] O. Bekers, J.H. Beijnen, B.J. Vis, A. Suenaga, M. Otagiri, A. Bult, W.J.M. Underberg, *Int. J. Pharm.* **1991**, *72*, 123-130.
- [23] X. Xu, L. Li, Z. Zhou, W. Sun, Y. Huang, *Int. J. Pharm.* **2016**, *507*, 50-60.
- [24] L. Lv, K. Qiu, X. Yu, C. Chen, F. Qin, Y. Shi, J. Ou, T. Zhang, H. Zhu, J. Wu, *et al.*, *J. Biomed. Nanotechnol.* **2016**, *12*, 973-85.
- [25] J.-K. Sun, K.-F. Ren, L.-Z. Zhu, J. Ji, *Colloids and Surfaces B: Biointerfaces* **2013**, *112*, 67-73.
- [26] Z. Liu, X. Sun, N. Nakayama-Ratchford, H. Dai, *ACS Nano* **2007**, *1*, 50-56.
- [27] Z. Chen, D. Pierre, H. He, S. Tan, C. Pham-Huy, H. Hong, J. Huang, *Int. J. Pharm.* **2011**, *405*, 153-161.
- [28] H. Bakirci, A.L. Koner, M.H. Dickman, U. Kortz, W.M. Nau, *Angew. Chem., Int. Ed.* **2006**, *4*, 7400-7404.
- [29] L. Baldini, A. Casnati, F. Sansone, R. Ungaro, *Chem. Soc. Rev.* **2007**, *36*, 254-266.
- [30] A.R. Mustafina, V.V. Skripacheva, A.T. Gubaidullin, S.K. Latipov, A.V. Toropchina, V. V. Yanilkin, S.E. Solovieva, I.S. Antipin, A.I. Konovalov, *Inorg. Chem.* **2005**, *44*, 4017-4023.
- [31] G.G. Talanova, V.S. Talavov, H.-S. Hwang, C. Park, K. Surowiec, R. Bartsch, *Org. Biomol. Chem.* **2004**, *2*, 2585-2592.
- [32] K. Wang, D.-S. Guo, Y. Liu, *Chem. Eur. J.* **2010**, *16*, 8006 - 8011.
- [33] K. Wang, D.-S. Guo, X. Wang, Y. Liu, *ACS Nano* **2011**, *5*, 2880-2894.
- [34] P. Job, *Ann. Chim.* **1928**, *9*, 113-203.
- [35] M. Airoldi, G. Barone, G. Gennaro, A.M. Giuliani, M. Giustini, *Biochem.* **2014**, *53*, 2197-2207.
- [36] F.M. Menger, C.E. Portnoy, *J. Am. Chem. Soc.* **1967**, *89*, 4698-4703.
- [37] C. Pérez-Arnaiz, N. Busto, J.M. Leal, B. García, *J. Phys. Chem. B* **2014**, *118*, 1288-1295.
- [38] G. Ercolani, *J. Am. Chem. Soc.* **2003**, *25*, 16097-16103.
- [39] A.A. Saboury, A. A. Moosavi-Movahedi, *Biochem. Educ.* **1994**, *22*, 48-49.
- [40] P. López-Cornejo, P. Pérez, F. García, R. de la Vega, F. Sánchez, *J. Am. Chem. Soc.* **2002**, *124*, 5154-5164.
- [41] H. E. Gottlieb, V. Kotlyar, A. Nudelman, *J. Org. Chem.* **1997**, *62*, 7512-7515.
- [42] B. Allart, P. Lehtolainen, S. Ylä-Herttuala, J.F. Martín, D.L. Selwood, *Bioconjugate Chem.* **2003**, *14*, 187-194.
- [43] J. van Meerloo, G.J.L. Kaspers, J. Cloos, *Methods Mol. Biol.* **2011**, *731*, 237-45.

**Entry for the Table of Contents** (Please choose one layout)

Layout 1:

## FULL PAPER

Encapsulation of free doxorubicin molecules in solution diminishing their side effects.



*F. J. Ostos, J. A. Lebrón,<sup>1</sup> M. L. Moyá, M.<sup>1</sup> López-López, A. Sánchez, A. Clavero, C.B. García-Calderón, I.V. Rosado and P. López-Cornejo\**

*Page No. – Page No.*

**USE OF P-SULFOCALIX[6]ARENE AS NANOCARRIER FOR DOXORUBICIN CONTROLLED DELIVERY**